Journal of Organometallic Chemistry 880 (2019) 261–266

Contents lists available at ScienceDirect

Journal of Organometallic Chemistry

journal homepage: www.elsevier.com/locate/jorganchem

Synthesis of highly branched polyethylene using para-benzhydryl substituted iminopyridyl Ni(II) and Pd(II) complexes

Ruiping Li [a, 1], Jinlong Sun [a, 1], Susu Tian [a], Yang Zhang [a], Dengfeng Guo [a], Weimin Li [a, *], Fuzhou Wang [b, **]

[a] Advanced Catalysis and Green Manufacturing Collaborative Innovation Center, School of Petrochemical Engineering, Changzhou University, Changzhou, 213164, China
[b] Institute of Physical Science and Information Technology, Anhui University, Hefei, 230601, Anhui, China

ARTICLE INFO

Article history:
Received 29 September 2018
Received in revised form
13 November 2018
Accepted 16 November 2018
Available online 17 November 2018

Keywords:
Ni(II) and Pd(II) complexes
Iminopyridyl
Chain-walking
Ethylene oligo-/polymerization
Highly branched

ABSTRACT

A series of *para*-benzhydryl substituted iminopyridyl-based Ni(II) and Pd(II) complexes with systematically varied ligand steric, [2,6-R_2-4-$CHPh_2C_6H_2N=CH(NC_6H_5)$]$MX_2$ (MX_2 = $NiBr_2$ or $PdCl_2$; R = -$CHPh_2$ (**Ni1**,**Pd1**); R = ^{i}Pr (**Ni2**,**Pd2**); R = Et (**Ni3**,**Pd3**); R = Me (**Ni4**,**Pd4**)], were synthesized and applied to ethylene oligo-/polymerization in combination with methylaluminoxane (MAO). These Ni(II) catalysts displayed good thermal stability and high activity of up to 7.13×10^6 g PE (mol Ni h)$^{-1}$, while the Pd(II) catalysts produced highly branched oligomers in high yields. Specifically, methyl-substituted complex **Pd4** exhibited higher activities and produced highly branched polyethylene (up to 141 branches/1000C). The branching densities were increased with increasing the polymerization temperature and decreasing the ligand bulkiness, and could be tuned over the wide range of 95–141/1000C. However, the molecular weights of the produced polymers follow the opposite trend.

1. Introduction

Polyolefin-based materials have been playing pivotal roles in today's polymer industry as well as in our daily lives [1]. In recent years, the interest in highly branched ethylene oligomers [2–4] increased obviously because of their unique physical properties and potential applications as lubricants, adhesives, and paints. The cationic Ni(II) and Pd(II) catalysts [5–17] for olefin polymerization has received extensive researches owing to the precise control of branching microstructure, molecular weights and properties of the resulting polyolefins [18–40]. There are many papers for ethylene polymerization using N-N bi-dentate pre-catalysts ligated by α-diimine [41–52], iminopyridyl [53,54], iminopyrrolyl [55], and many others. More importantly, the iminopyridyl-based Ni(II) and Pd(II) pre-catalysts [56–59] are able to polymerize ethylene to afford low molecular-weight branched oligomers, and their catalytic activities are high more than those of Brookhart-type α-diimine catalysts.

Many pyridinylimine-type catalysts incorporating a single *ortho*-substituted aryl imine structure have been reported (Chart 1 I-IV) [56–60]. For example, Sun et al. reported that a series of dibenzhydryl substituted 2-iminopyridyl nickel catalysts **I** with different substituents (R_2 = H, Me) showed high catalytic activities in ethylene polymerization of up to 10^7 g PE (mol Ni h)$^{-1}$ [56], but only produced branched polyethylene with low molecular weight of less than 1000 g mol^{-1}. The steric bulky **I** remained high activity toward ethylene polymerization (ca. 10^6 g PE (mol Ni h)$^{-1}$) [57], but the obtained polyethylenes were now short chain oligomers. Recently, Gao et al. synthesized two iminopyridyl-based palladium complexes **II** with dibenzhydryl substituents [58]. Their cationic iminopyridyl-based palladium complexes were capable of catalyzing ethylene oligomerization with good activities, and produced highly branched oligomers with molecular weights of 600–800 g mol^{-1} and narrow polydispersities (1.03–1.12). The introduction of bulky *ortho*-benzhydryl enhanced catalytic activity, thermal stability of the catalyst, and molecular weight of the obtained products. Brookhart et al. reported that 8-arylnaphthyl groups incorporated into pyridine-imine nickel catalysts **III** that block only a single axial site were highly effective in retarding chain transfer [59]. These catalysts produced branched polyethylenes (ca. 30–90 branches per 1000 carbons) with good molecular weight up to 2.6×10^4 g mol^{-1}. Chen et al. reported that a series of

* Corresponding author.
** Corresponding author.
E-mail addresses: liweimin@cczu.edu.cn (W. Li), wangfuzhou1718@126.com (F. Wang).
[1] Ruiping Li and Jinlong Sun contribute equally to the article.

https://doi.org/10.1016/j.jorganchem.2018.11.024
0022-328X/

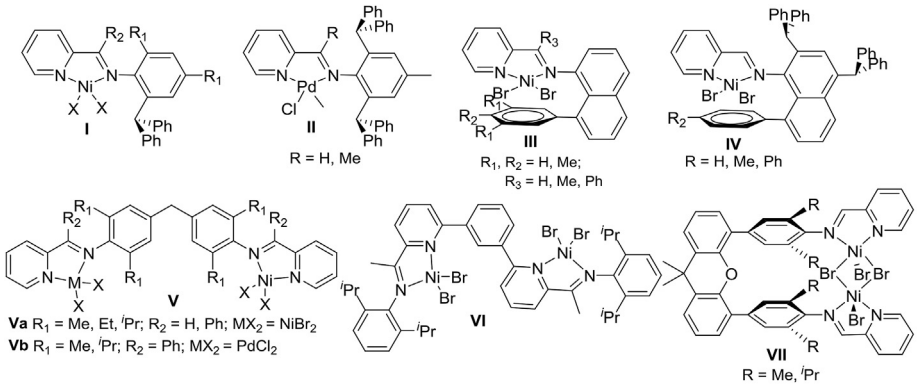

Chart 1. Selected examples of iminopyridyl-based Ni(II) and Pd(II) catalysts.

iminopyridyl nickel catalysts **IV** containing both the dibenzhydryl and the naphthyl moieties polymerized ethylene with high activity and high thermal stability [60], and also generated semicrystalline poly(α-olefin)s with high melting temperatures.

Dinuclear iminopyridyl Ni(II) and Pd(II) complexes (Chart 1 V-VII) have been explored in catalysis with the potential of cooperative effects between two proximate active metal centers, including the applications in ethylene polymerization [61–64]. For example, Sun et al. designed some methylene-bridged dinuclear nickel catalysts **Va** with bis-iminopyridine ligands [61]. These catalysts showed good activities for ethylene oligomerization and polymerization in the presence of MAO, and produced mixtures of oligomers and polyethylenes. The Ni—Ni cooperativity effect may be responsible for the unique properties of these dinuclear catalysts. Hu et al. reported that some bridged dinuclear diimine nickel and palladium complexes (**Vb**) catalyzed the vinyl addition polymerization of norbornene at a single active site with high activity [62]. The latter exhibited higher activity than the former. The packing density, thermos stability, and the glass transition temperatures of copolymers are increased relative to polystyrene. The solubility and process ability of copolymers are improved relative to polynorbornene. Solan et al. also synthesized an aryl-bridged pyridineimine palladium complex **VI** which showed some activity for ethylene oligomerization, and produced low molecular weight polyethylene with methyl-branched products predominating for this nickel systems [63].

Our group designed two xanthene-bridged iminopyridyl dinuclear nickel complexes **VII** with two Ni centers connected by two bromide bridges [64]. The iminopyridyl dinuclear nickel complexes activated by MAO showed higher catalytic activities of up to 2.2×10^6 g PE (mol Ni h)$^{-1}$, higher molecular weights, and produced polyethylene with much lower branching density (27/1000C) than their mononuclear analogues. These results clearly demonstrated the great potentials of dinuclear nickel catalysts with the xanthene-bridged coordination modes in controlling the ethylene polymerization process as well as the microstructures of the resulting polyethylene products. In this work, we report the applications of a class of *para*-dibenzhydryl substituted iminopyridyl-based Ni(II) and Pd(II) complexes with systematically varied ligand sterics, and study the effect of ligand structure and polymerization conditions on ethylene oligo-/polymerization in detail.

2. Experimental

2.1. General considerations

Experiments involving air- and/or moisture-sensitive materials were carried out under a dry nitrogen atmosphere using a glovebox, dual vacuum/nitrogen lines and standard Schlenk techniques. Deuterated solvents for NMR spectroscopy were dried and distilled prior to use. The NMR spectra were recorded on a Bruker Ascend 400 spectrometer at ambient temperature unless otherwise stated. The chemical shifts of the ^{1}H and ^{13}C NMR spectra were referenced to tetramethylsilane (TMS). Molecular weights and molecular weight distributions were determined by gel permeation chromatography (GPC) at 150 °C using a PL-GPC 220 high-temperature GPC system. Elemental analysis was performed by the Analytical Center of the Changzhou University. Single crystal of the nickel complex was got by slow diffusion of *n*-hexane into CH_2Cl_2 at room temperature. X-ray crystallography analysis was performed on an Oxford Diffraction Gemini S Ultra CCD diffraction meter equipped with mirro Cu Kα ($\lambda = 1.54184$ Å) radiation at room temperature. Toluene, CH_2Cl_2, THF, and *n*-hexane were purified over 4 Å molecular sieves. All *para*-benzhydryl derivatives were prepared according to reported procedures [54]. Dichloromethane, toluene, and hexanes were purified by solvent purification systems. All other reagents were purchased from commercial sources and used without purification.

2.2. General synthesis of the para-benzhydryl substituted iminopyridyl ligands L1–L4

2.2.1. Synthesis of (2,4,6-tribenzhydrylphenylimino)pyridine (*L1*)

In a 100 mL flask, formic acid (0.2 mL) was added in to the stirred solution of picolinaldehyde (0.21 g, 2.00 mmol) and 2,4,6-tribenzhydrylaniline (1.18 g, 2.00 mmol) in ethanol (30 mL). The mixture stirred for 12 h at 50 °C, then cooled and the precipitate was separated by filtration to afford yellow solid. This obtained solid was purified by recrystallization with a mixture of EtOH/CH_2Cl_2, washed with cold ethanol and dried under vacuum to obtain yellow powder (1.21 g, 89% yield). ^{1}H NMR (400 MHz, $CDCl_3$, ppm): δ 8.57 (d, $J = 7.4$ Hz, 1H, N=C*H*C$_5$H$_5$N), 7.72–7.64 (m, 2H, Py–*H*), 7.30–7.24 (m, 2H, Py–*H*), 7.19–6.89 (m, 30H, Ph–*H*), 6.67 (s, 2H, Ar–*H*), 5.41 (s, 1H, –C*H*Ph$_2$), 5.30 (s, 2H, –C*H*Ph$_2$). ^{13}C NMR (100 MHz, $CDCl_3$, ppm): δ 165.1 (N=*C*HPy), 153.6, 149.6, 148.5, 144.3, 143.5, 138.3, 136.3, 130.0, 129.5, 129.4, 129.2, 128.1, 128.0, 126.1, 126.0, 125.1, 122.0, 56.2 (–*C*HPh$_2$), 51.9 (–*C*HPh$_2$). Anal. Calcd. for $C_{51}H_{40}N_2$: C, 89.96; H, 5.92; N, 4.11. Found: C, 89.83; H, 5.78; N, 4.38. FT-IR (KBr): 1647 cm^{-1} ($\nu_{C=N}$).

2.2.2. Synthesis of (4-benzhydryl-2,6-diisopropylphenylimino) pyridine (*L2*)

L2 was prepared in a similar synthetic procedure to that for **L1** as yellow powder (0.80 g, 92% yield). ^{1}H NMR (400 MHz, $CDCl_3$, ppm): δ 8.75 (d, $J = 7.8$ Hz, 1H, Py–*H*), 8.36 (s, 1H, N=C*H*C$_5$H$_5$N), 8.29 (d, $J = 7.2$ Hz, 1H, Py–*H*), 7.88–7.84 (m, 1H, Py–*H*), 7.44–7.41

(m, 1H, Py−*H*), 7.34–7.29 (m, 4H, Ph−*H*), 7.26–7.23 (m, 2H, Ph−*H*), 7.19 (d, $J = 7.9$ Hz, 4H, Ph−*H*), 6.94 (s, 2H, Ar−*H*), 5.56 (s, 1H, −C*H*Ph$_2$), 2.96 (s, 2H, −C*H*(CH$_3$)$_2$), 1.11 (d, $J = 7.3$ Hz, 12H, −C*H*$_3$). ^{13}C NMR (100 MHz, $CDCl_3$, ppm): δ 163.0 (N=*C*HPy), 154.5, 149.7, 146.5, 144.5, 139.5, 137.1, 136.8, 129.5, 128.2, 126.1, 125.3, 124.3, 121.3, 56.9 (−*C*HPh$_2$), 28.0 (−*C*H$_3$), 24.5 (−*C*H(CH$_3$)$_2$). Anal. Calcd. for $C_{31}H_{32}N_2$: C, 86.07; H, 7.46; N, 6.48. Found: C, 86.21; H, 7.02; N, 6.77. FT-IR (KBr): 1648 cm^{-1} ($\nu_{C=N}$).

2.2.3. Synthesis of (4-benzhydryl-2,6-diethylphenylimino)pyridine (*L3*)

L3 was prepared in a similar synthetic procedure to that for **L1** as yellow powder (0.77 g, 95% yield). ^{1}H NMR (400 MHz, $CDCl_3$, ppm): δ 8.71 (d, $J = 7.8$ Hz, 1H, Py−*H*), 8.35 (s, 1H, N=C*H*C$_5$H$_5$N), 8.26 (d, $J = 7.8$ Hz, 1H, Py−*H*), 7.85–7.81 (m, 1H, Py−*H*), 7.42–7.37 (m, 1H, Py−*H*), 7.33–7.15 (m, 10H, Ph−*H*), 6.85 (s, 2H, Ar−*H*), 5.52 (s, 1H, −*CH*Ph$_2$), 2.49–2.41 (m, 4H, −*CH*$_2$CH$_3$), 1.06 (t, $J = 7.5$ Hz, 6H, −*CH*$_3$). ^{13}C NMR (100 MHz, $CDCl_3$, ppm): δ 163.0 (N=*C*HPy), 154.5, 149.6, 147.7, 144.4, 139.6, 136.8, 132.7, 129.5, 128.3, 127.5, 126.2, 125.3, 121.1, 56.6 (−*C*HPh$_2$), 24.8 (−*C*H$_2$CH$_3$), 14.5 (−*C*H$_3$). Anal. Calcd. for $C_{29}H_{28}N_2$: C, 86.10; H, 6.98; N,6.92. Found: C, 85.89; H, 7.38; N,6.73. FT-IR (KBr): 1646 cm^{-1} ($\nu_{C=N}$).

2.2.4. Synthesis of (4-benzhydryl-2,6-dimethylphenylimino) pyridine (*L4*)

L4 was prepared in a similar synthetic procedure to that for **L1** as yellow powder (0.68 g, 90% yield). ^{1}H NMR (400 MHz, $CDCl_3$, ppm): δ 8.71 (d, J = 7.6 Hz, 1H, Py−*H*), 8.35 (s, 1H, N=C*H*C$_5$H$_5$N), 8.27 (d, J = 7.8 Hz, 1H, Py−*H*), 7.86–7.81 (m, 1H, Py−*H*), 7.42–7.37 (m, 1H, Py−*H*), 7.31–7.17 (m, 10H, Ph−*H*), 6.83 (s, 2H, Ar−*H*), 5.49 (s, 1H, −*CH*Ph$_2$), 2.10 (s, 6H, −*CH*$_3$). ^{13}C NMR (100 MHz, $CDCl_3$, ppm): δ 163.4 (N=*C*HPy), 154.5, 149.6, 148.5, 144.2, 139.5, 136.7, 129.5, 129.2, 128.3, 126.9, 126.1, 125.3, 121.2, 56.4 (−*C*HPh$_2$), 18.5 (−*C*H$_3$). Anal. Calcd. for $C_{27}H_{24}N_2$: C, 86.13; H, 6.43; N, 7.44. Found: C, 86.52; H, 6.12; N, 7.36. FT-IR (KBr): 1647 cm^{-1} ($\nu_{C=N}$).

2.3. General method for the synthesis of dibromide nickel complexes

All nickel complexes were obtained in a similar synthetic procedure by the reaction of the corresponding ligands with (DME) $NiBr_2$ (DME = 1,2-dimethoxyethane) in CH_2Cl_2. A typical synthetic way of **Ni1**−**Ni4** is as follows: (DME)$NiBr_2$ (0.31 g, 1.0 mmol), ligand (1.0 mmol) and CH_2Cl_2 (25 mL) were combined in a 100 mL Schlenk flask under an atmosphere of nitrogen. After stirred for 12 h at room temperature, and the resulting suspension was filtered. The reaction solution was evaporated to dryness under vacuum and washed three times by diethyl ether (3 × 14 mL), and then dried under vacuum to obtain complex as a brown solid powder.

(**^{diPhCH}N^N-Py)L1NiBr$_2$** (**Ni1**) (0.80 g, 93%): Anal. Calcd for $C_{51}H_{40}Br_2N_2Ni$: C, 68.11; H, 4.48; N, 3.11. Found: C, 68.29; H, 4.52; N, 2.99. FT-IR (KBr): 1625 cm^{-1} ($\nu_{C=N}$).

(**$^{i\text{-}Pr}$N^N-Py)L2NiBr$_2$** (**Ni2**) (0.61 g, 94%): Anal. Calcd for $C_{31}H_{32}Br_2N_2Ni$: C, 57.18; H, 4.95; N, 4.30. Found: C, 57.32; H, 4.84; N, 4.27. FT-IR (KBr): 1623 cm^{-1} ($\nu_{C=N}$).

(**^{Et}N^N-Py)L3NiBr$_2$** (**Ni3**) (0.60 g, 96%): Anal. Calcd for $C_{29}H_{28}Br_2N_2Ni$: C, 55.90; H, 4.53; N, 4.50. Found: C, 56.06; H, 4.49; N, 4.38. FT-IR (KBr): 1622 cm^{-1} ($\nu_{C=N}$).

(**^{Me}N^N-Py)L4NiBr$_2$** (**Ni4**) (0.56 g, 95%): Anal. Calcd for $C_{27}H_{24}Br_2N_2Ni$: C, 54.50; H, 4.07; N, 4.71. Found: C, 54.25; H, 4.13; N, 4.90. FT-IR (KBr): 1625 cm^{-1} ($\nu_{C=N}$).

2.4. General method for the synthesis of palladium complexes

All palladium complexes were prepared in a similar manner by the reaction of $(MeCN)_2PdCl_2$ with the corresponding ligands in CH_2Cl_2, respectively. A typical synthetic procedure of **Pd1**−**Pd4** is as follows: $(MeCN)_2PdCl_2$ (0.26 g, 1.0 mmol) and ligand (1.0 mmol) were placed in a Schlenk flask under N_2 atmosphere. CH_2Cl_2 (30 mL) was added, and the reaction mixture was stirred at room temperature for 24 h. The resulting suspension was filtered. The solvent was removed under vacuum and the residue was washed with diethyl ether (3 × 13 mL), and then dried under vacuum at room temperature to obtain a yellow solid powder.

(**^{diPhCH}N^N-Py)L1PdCl$_2$** (**Pd1**) (0.79 g, 92%): ^{1}H NMR (400 MHz, $CDCl_3$, ppm): δ 9.06 (d, $J = 7.4$ Hz, 1H, N=C*H*C$_5$H$_5$N), 8.24–7.91 (m, 2H, Py−*H*), 7.29–6.90 (m, 34H, Py−*H* and Ar−*H*), 6.55 (s, 2H, Ar−*H*), 5.56 (s, 1H, −*CH*Ph$_2$), 5.45 (s, 2H, −*CH*Ph$_2$). ^{13}C NMR (100 MHz, $CDCl_3$, ppm): δ 176.9 (N=*C*HPy), 154.7, 150.7, 144.8, 143.9, 143.8, 143.6, 143.5, 142.0, 138.3, 136.3, 130.9, 130.3, 130.1, 129.6, 129.0, 126.9, 126.7, 56.2 (−*C*HPh$_2$), 51.9 (−*C*HPh$_2$). Anal. Calcd for $C_{51}H_{40}Cl_2N_2Pd$: C, 71.38; H, 4.70; N, 3.26. Found: C, 71.49; H, 4.58; N, 3.27. FT-IR (KBr): 1623 cm^{-1} ($\nu_{C=N}$).

(**$^{i\text{-}Pr}$N^N-Py)L2PdCl$_2$** (**Pd2**) (0.57 g, 94%): ^{1}H NMR (400 MHz, $CDCl_3$, ppm): δ 9.07 (s, 1H, N=C*H*C$_5$H$_5$N), 8.80 (d, $J = 7.8$ Hz, 1H, Py−*H*), 8.42–8.00 (m, 3H, Py−*H*), 7.35–7.13 (m, 10H, Ph−*H*), 6.97 (s, 2H, Ar−*H*), 5.65 (s, 1H, −*CH*Ph$_2$), 3.22 (s, 2H, −*CH*(CH$_3$)$_2$), 1.18 (d, $J = 7.3$ Hz, 12H, −*CH*$_3$). ^{13}C NMR (100 MHz, $CDCl_3$, ppm): δ 175.5 (N=*C*HPy), 155.6, 151.2, 144.5, 143.7, 143.5, 142.1, 136.2, 130.6, 130.5, 129.5, 129.1, 126.9, 126.7, 56.0 (−*C*HPh$_2$), 18.3 (−*C*H$_3$). Anal. Calcd for $C_{31}H_{32}Cl_2N_2Pd$: C, 61.05; H, 5.29; N, 4.59. Found: C, 61.12; H, 5.34; N, 4.47. FT-IR (KBr): 1604 cm^{-1} ($\nu_{C=N}$).

(**^{Et}N^N-Py)L3PdCl$_2$** (**Pd3**) (0.54 g, 93%): ^{1}H NMR (400 MHz, $CDCl_3$, ppm): δ 9.06 (s, 1H, N=C*H*C$_5$H$_5$N), 8.71 (d, $J = 7.8$ Hz, 1H, Py−*H*), 8.42–7.99 (m, 3H, Py−*H*), 7.35–7.14 (m, 10H, Ph−*H*), 6.91 (s, 2H, Ar−*H*), 5.64 (s, 1H, −*CH*Ph$_2$), 2.71–2.59 (m, 4H, −*CH*$_2$CH$_3$), 1.14–1.08 (m, 6H, −*CH*$_3$). ^{13}C NMR (100 MHz, $CDCl_3$, ppm): δ 175.2 (N=*C*HPy), 155.4, 150.8, 144.2, 143.5, 143.3, 141.9, 136.0, 130.3, 130.2, 129.5, 128.9, 126.8, 126.5, 56.1 (−*C*HPh$_2$), 24.6 (−*C*H$_2$CH$_3$), 14.4 (−*C*H$_3$). Anal. Calcd for $C_{29}H_{28}Cl_2N_2Pd$: C, 59.86; H, 4.85; N, 4.81. Found: C, 59.82; H, 4.76; N, 4.94. FT-IR (KBr): 1621 cm^{-1} ($\nu_{C=N}$).

(**^{Me}N^N-Py)L4PdCl$_2$** (**Pd4**) (0.52 g, 95%): ^{1}H NMR (400 MHz, $CDCl_3$, ppm): δ 9.09 (s, 1H, N=C*H*C$_5$H$_5$N), 8.84 (d, J = 7.6 Hz, 1H, Py−*H*), 8.37–7.81 (m, 3H, Py−*H*), 7.33–7.13 (m, 10H, Ph−*H*), 6.84 (s, 2H, Ar−*H*), 5.51 (s, 1H, −*CH*Ph$_2$), 2.12 (s, 6H, −*CH*$_3$). ^{13}C NMR (100 MHz, $CDCl_3$, ppm): δ 175.4 (N=*C*HPy), 155.1, 150.6, 144.0, 143.3, 143.0, 141.7, 135.8, 130.1, 129.8, 129.1, 128.4, 126.5, 126.1, 56.0 (−*C*HPh$_2$), 18.3 (−*C*H$_3$). Anal. Calcd for $C_{27}H_{24}Cl_2N_2Pd$: C, 58.56; H, 4.37; N, 5.06. Found: C, 58.41; H, 4.45; N, 5.13. FT-IR (KBr): 1622 cm^{-1} ($\nu_{C=N}$).

2.5. X-ray structure determinations

Single crystals of complexes **Pd2** and **Pd3** suitable for X-ray analysis were obtained by dissolving the complex in CH_2Cl_2, following by slow layering of the resulting solution with *n*-hexane. Data collections were performed at 296(2) K on a Bruker SMART APEX diffractometer with a CCD area detector, using graphite monochromated Mo*Kα* radiation (λ = 0.71073 Å). The determination of crystal class and unit cell parameters was carried out by the SMART program package. The raw frame data were processed using SAINT and SADABS to yield the reflection data file. The structures were solved by using the SHELXTL program. Refinement was performed on F^2 anisotropically for all non-hydrogen atoms by the full-matrix least-squares method. The hydrogen atoms were placed at the calculated positions and were included in the structure calculation without further refinement of the parameters. Crystal data, data collection, and refinement parameters are listed in Table S1.

2.6. Catalytic ethylene oligo-/polymerization tests

In a typical experiment, a 100 mL glass thick-walled pressure vessel was charged with required amount of MAO, 50 mL toluene and a magnetic stir bar in the glovebox. The pressure vessel was connected to a high pressure polymerization line and the solution was degassed. The vessel was warmed to the desired temperature using an oil bath and allowed to equilibrate for 15 min. Then Ni(II) or Pd(II) complexes in 2 mL CH_2Cl_2 was injected into the vessel via syringe. With rapid stirring, the reactor was pressurized and maintained at 6.0 atm of ethylene. After the desired amount of polymerization time, the vessel was vented and terminated in 5% acidified methanol. The polymers obtained were adequately washed with methanol and dried under vacuum at 50 °C for 12 h.

3. Results and discussion

3.1. Synthesis and characterization of the Ni(II) and Pd(II) complexes

The desired *para*-benzhydryl derivatives were prepared using the literature procedure in high yields. The *para*-benzhydryl substituted iminopyridyl ligands and the corresponding pre-catalysts used in this study are summarized in Scheme 1. The *para*-benzhydryl substituted iminopyridyl ligands **L1**–**L4** were prepared by the condensation of equivalents of the appropriate aniline with one equivalent of picolinaldehyde, usually in the presence of a formic acid catalyst. Equimolar amounts of $NiBr_2$(DME) or $(CH_3CN)_2PdCl_2$ and the corresponding ligands **L1**–**L4** in CH_2Cl_2 gave catalyst precursors complexes **Ni1**–**Ni4** and **Pd1**–**Pd4** in almost quantitative yields, respectively. These compound formulations were characterized by elemental analysis, FT-IR and NMR spectroscopy. The fitted elemental analysis of complexes **Pd2** and **Pd3** fits the molecular structures obtained by the X-ray structural studies (see below).

3.2. X-ray crystallographic studies

Suitable crystal of Pd(II) complexes **Pd2** and **Pd3** were obtained by layering *n*-hexane onto their dichloromethane solution at room temperature. The molecular structures of complexes **Pd2** and **Pd3** were confirmed by single-crystal X-ray diffraction and the corresponding ORTEP diagram with selected bond distances and angles are shown in Fig. 1. Crystal data, data collection and refinement parameters are listed in Table S1 (see Supporting Information). The structure of complexes **Pd2** and **Pd3** showed the expected bidentate coordination of the iminopyridyl nitrogen atoms to the Pd center, forming distorted square-planar coordination environments. The bond distances and angles are typical and similar with reported complex **II** [58]. The systematic tuning of the *ortho*-R substituted ligand steric coordination environment can be clearly observed by these molecular structures, expectantly to tune the catalytic activity for olefin polymerization and to control the polymer microstructures.

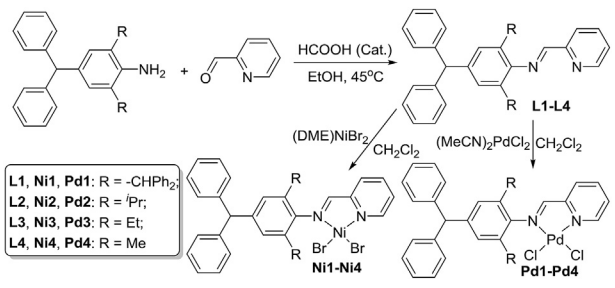

Scheme 1. Synthesis of iminopyridyl-based Ni(II) complexes **Ni1**–**Ni4** and Pd(II) complexes **Pd1**–**Pd4**.

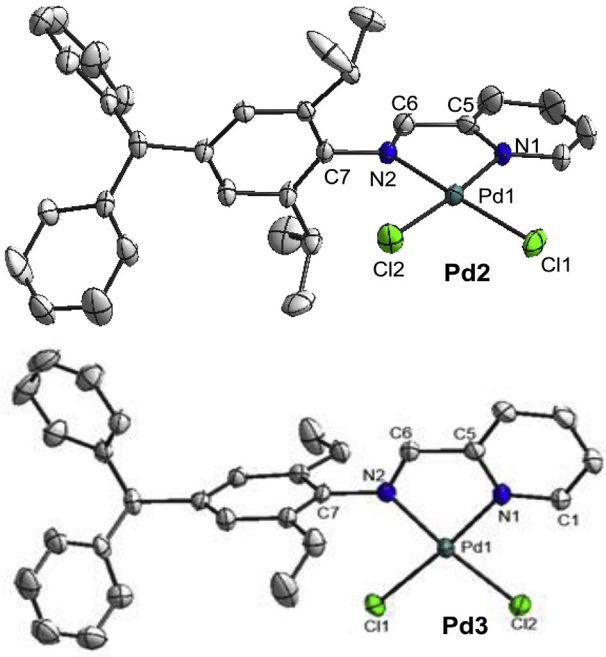

Fig. 1. Molecular structure of complexes **Pd2** and **Pd3** with thermal ellipsoids drawn at 30% probability, and H atoms have been omitted for clarity. Selected bond lengths (Å) and angles (°) for complexes: (**Pd2**) Pd1–N2, 2.004(6); Pd1–N1, 2.047(7); Pd1–Cl2; 2.273(3); Pd1–Cl1, 2.285(2); N2–Pd1–N1, 80.4(3); Cl2–Pd1–Cl1, 91.59(11); N1–Pd1–Cl1, 95.3(2); N1–Pd1–Cl2, 172.8(2). (**Pd3**) Pd1–N1, 2.019(3); Pd1–N2, 2.016(3); Pd1–Cl, 2.272(11); Pd1–Cl2, 2.296(11); Cl1–Pd1–Cl2, 90.75(4); N2–Pd1–Cl2, 174.47(10); N2–Pd1–Cl1, 94.41(10); N2–Pd1–N1, 80.50(13).

3.3. Ethylene polymerization studies

Sun et al. studied the effect of various co-catalysts on ethylene polymerization using corresponding dibenzhydryl substituted 2-iminopyridyl nickel catalysts **I** [56], MAO was the most effective co-catalyst among these alkylaluminium reagents and the catalytic system exhibited highest catalytic activities. Therefore, polymerizations of ethylene with Ni(II) complexes **Ni1**–**Ni4** activated by MAO with the [Al]/[Ni] ratio of 600 were carried out at various polymerization temperatures and steric effects for 30 min under 6 atm of ethylene, and the results are listed in Table 1.

The influence of the polymerization temperature was investigated by varying the temperature from 20 to 60 °C. The maximum catalytic activities of complexes **Ni1**–**Ni4** were observed at 40 °C (Table 1, entries 2, 5, 8 and 11). This polymerization at 60 °C, the catalytic activities of the *para*-benzhydryl substituted complexes **Ni1**–**Ni4** still maintained good catalytic activities on the level of 5.24×10^6 g of PE/(mol Ni h), and showed much higher thermal stability than the corresponding methyl substituted complex **C4** (Table 1, entries 3, 6, 9 and 12). The lower activities at higher temperatures should be ascribed to the partial deactivation of the active species and the lower solubility of ethylene in toluene at elevated temperatures [65].

The effect of catalyst precursors **Ni1**–**Ni4** were investigated at various polymerization temperatures. These Ni(II) complexes produced polymers in high yields with low molecular weights over a very wide range ($(2.3–11.3) \times 10^3$ g/mol) and narrow molecular

Table 1
Catalytic results of ethylene polymerization with complexes **Ni1**–**Ni4**.[a]

Entry	Precat.	T (°C)	Yield (g)	Activity[b]	M_n[c] (10^3)	M_w/M_n[c]	B[d]
1	**Ni1**	20	6.42	5.14	11.27	1.58	95
2	**Ni1**	40	7.81	6.25	10.32	1.36	101
3	**Ni1**	60	5.91	4.73	8.76	1.91	108
4	**Ni2**	20	7.34	5.87	9.02	1.75	100
5	**Ni2**	40	8.52	6.82	5.38	1.70	105
6	**Ni2**	60	6.07	4.86	4.14	1.92	113
7	**Ni3**	20	7.84	6.27	6.90	1.76	104
8	**Ni3**	40	8.91	7.13	5.00	1.84	111
9	**Ni3**	60	7.13	5.70	3.52	2.31	124
10	**Ni4**	20	6.84	5.47	5.15	1.69	110
11	**Ni4**	40	7.68	6.14	3.99	1.72	126
12	**Ni4**	60	6.55	5.24	2.31	2.63	131

[a] Polymerization conditions: Ni = 2.5 μmol in CH_2Cl_2 (2 mL); cocatalyst MAO, [Al]/[Ni] = 600; solvent = toluene (50 mL); 6.0 atm of ethylene; time = 30 min.
[b] 10^6 g of PE (mol of Ni)$^{-1}$ h^{-1}.
[c] M_n and M_w/M_n determined by GPC, 10^3 g mol^{-1}.
[d] Branching density, branches/1000C = $(CH_3/3)/[(CH + CH_2 + CH_3)/2] \times 1000$, determined by ^{1}H NMR analysis [6].

weight distributions (M_w/M_n = 1.36–2.63). Steric effect of *ortho*-position in anilinic moiety can be evaluated by comparing **Ni1** to **Ni4** (Table 1). For example, the complex **Ni3** with ethyl gourps showed the highest activity among these complexes of up to 7.13×10^6 g of PE/(mol Ni h) (entries), but gave the lower molecular weight than that of complex **Ni2** (Table 1, entries 5 *vs* 8). The highest molecular weight of the polymers obtained by **Ni1** indicated that the rate of chain propagation was greatly promoted by the bulky *ortho*-benzhydryl substituents of the ligand's aryl rings, which should suppress chain-transfer reactions, and is consistent with the literature [56]. This result indicated that the molecular weight was increased with increasing the bulkiness of the ligand [-$CHPh_2$ > ^{i}Pr > Et > Me].

Polymerizations of ethylene with Pd(II) complexes **Pd1**–**Pd4** activated by MAO were also carried out at various steric effects and polymerization temperatures for 3 h, and the results are listed in Table 2. Compared with corresponding palladium catalysts **II** [58], these catalytic systems showed good activities (ca. 10^5 g PE (mol Pd h)$^{-1}$). The maximum catalytic activity of **Pd1**–**Pd4** was observed at 40 °C (Table 2, entries 2, 5, 8 and 11). Moreover, the catalytic activities of the Pd(II) catalysts and M_n values of polymers are lower than that of the corresponding Ni(II) catalysts (Table 2 *vs* 1). The rates of polymerization were decreased as the steric bulk of the *ortho*-substituents on the iminopyridyl ligand increases. However, the molecular weights of the produced polymers follow the opposite trend.

Table 2
Catalytic results of ethylene polymerization with complexes **Pd1**–**Pd4**.[a]

Entry	Precat.	T (°C)	Yield (g)	Activity[b]	M_n[c]	M_w/M_n[c]	B[d]
1	**Pd1**	20	2.14	1.43	2930	1.61	101
2	**Pd1**	40	2.72	1.81	2790	1.69	105
3	**Pd1**	60	1.65	1.01	940	2.05	113
4	**Pd2**	20	2.48	1.65	1930	1.55	106
5	**Pd2**	40	3.07	2.05	1570	1.67	110
6	**Pd2**	60	2.13	1.42	790	2.33	117
7	**Pd3**	20	2.78	1.85	1580	1.85	109
8	**Pd3**	40	3.57	2.38	1270	1.70	121
9	**Pd3**	60	2.31	1.54	590	2.58	131
10	**Pd4**	20	2.89	1.93	950	2.02	125
11	**Pd4**	40	3.61	2.41	850	2.15	134
12	**Pd4**	60	2.45	1.63	570	3.79	141

[a] Polymerization conditions: Pd = 5 μmol in CH_2Cl_2 (2 mL); cocatalyst MAO, [Al]/[Pd] = 600; solvent = toluene (50 mL); 6.0 atm of ethylene; time = 3 h.
[b] 10^5 g of PE (mol of Pd)$^{-1}$ h^{-1}.
[c] M_n and M_w/M_n determined by GPC, g mol^{-1}.
[d] Branching density, branches/1000C = $(CH_3/3)/[(CH + CH_2 + CH_3)/2] \times 1000$, determined by ^{1}H NMR analysis [6].

3.4. Structure of the resulting polymers

The ^{1}H NMR analysis (Tables 1 and 2) [67,68] showed that the polyethylene branching structures was strong dependent on the polymerization temperatures and ligand structures [3]. For example, the branching degrees of resulting PEs were increased with polymerization temperatures from 20 to 60 °C, and the branching densities could be tuned over a very wide range (**Ni1**, 95–108/1000C; **Ni2**, 100–113/1000C; **Ni3**, 106–124/1000C; **Ni4**, 110–131/1000C; **Pd1**, 101–113/1000C; **Pd2**, 106–117/1000C; **Pd3**, 109–131/1000C; **Pd4**, 125–141/1000C). These substituted iminopyridyl catalysts with *para*-benzhydryl group afforded branched polyethylenes with a considerably higher branching degree than the corresponding classic iminopyridyl catalysts [53]. Besides, the branching densities obtained with Pd(II) catalysts were obviously higher than that of Ni(II) catalysts, which increased with decreasing the bulkiness of ligand. For example, at 40 °C, the number of chain branching was depended on the pre-catalysts and decreased in the following order, **Pd4** [Me, 134/1000C] > **Pd3** [^{i}Pr, 121/1000C] > **Pd2** [Et, 110/1000C] > **Pd1** [-$CHPh_2$, 105/1000C] (Table 2, entries 2, 5, 8 and 11).

The polymerization of ethylene with *para*-benzhydryl substituted iminopyridyl complexes **Ni1**–**Ni4** and **Pd1**–**Pd4** typically provides highly branched amourphous polyethylene through fast chain-walking mechanism. The chain branching distribution of the obtained branched polyethylenes was determined by ^{13}C NMR spectroscopy analysis [68,69]. For example, Figure S11 (Table 1, entry 1) showed that the obtained polyethylene with 95 branches/1000C using **Ni1** at 20 °C possessed 69 methyl, 5 ethyl, 2 *n*-propyl, 3 *n*-butyl, 1 sec-butyl and 15 longer chains (>C4 branches), among branches was predominately methyl. The branching structures of the polyethylene produced by **Pd4** at 60 °C (Fig. 2) showed that 78 methyl, 16 ethyl, 4 *n*-propyl, 8 *n*-butyl, 14 sec-butyl (branch on branch structure) and 21 longer chains (>C5 branches) exist for the amorphous polyethylene with highly branches up to 141 branches/1000C (Table 2, entry 12).

4. Conclusions

In summary, oligo-/polymerization of ethylene was catalyzed by a class of *para*-benzhydryl substituted iminopyridyl Ni(II) and Pd(II) complexes bearing different *ortho*-substituted groups (-$CHPh_2$, ^{i}Pr, Et and Me) activated by MAO. The introduction of *para*-benzhydryl group of the N-aryl substituents may promote the fast chain-walking process by the electronic effect in ethylene polymerization, which results in the good thermal stability, high catalytic

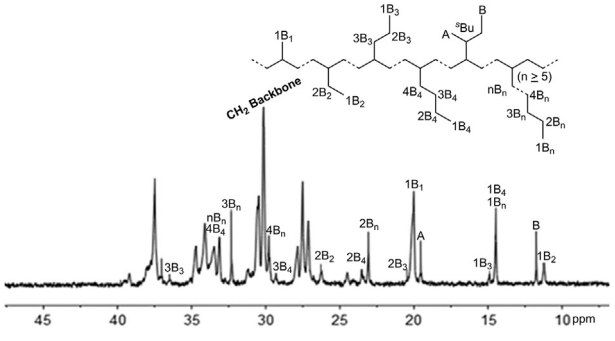

Fig. 2. ^{13}C NMR spectrum of polyethylene obtained by **Pd4** at 60 °C (Table 2, entry 12).

activity and produced highly branched polyethylenes. The results indicated the catalytic activities, the molecular weights and branching densities (97–141/1000C) could be tuned over a very wide range, depending on the catalyst structure and polymerization temperature. These Ni(II) catalytic systems displayed higher activity of up to 7.13×10^6 g PE (mol Ni h)$^{-1}$, while the Pd(II) catalytic systems produced highly branched oligomers in high yields. Specifically, methyl-substituted complex **Pd4** produced highly branched polyethylene of up to 141 branches/1000C.

Acknowledgements

This work was supported by National Natural Science Foundation of China (Grant No. 21801002), Advanced Catalysis and Green Manufacturing Collaborative Innovation Center (ACGM2016-06-01), Fundamental Research Funds for the Central Universities (WK2060200025) and Yixing Taodu Ying Cai Program.

Appendix A. Supplementary data

Supplementary data to this article can be found online at https://doi.org/10.1016/j.jorganchem.2018.11.024.

References

[1] D.B. Malpass, Introduction to Industrial Polyethylene, Wiley, Hoboken, NJ, 2010.
[2] Y. Chen, L. Wang, H. Yu, Y. Zhao, R. Sun, G. Jing, J. Huang, H. Khalid, N.M. Abbasi, M. Akram, Prog. Polym. Sci. 45 (2015) 23–43.
[3] L.H. Guo, S.Y. Dai, X.L. Sui, C.L. Chen, ACS Catal. 6 (2016) 428–441.
[4] L. Falivene, T. Wiedemann, I. GöttkerSchnetmann, L. Caporaso, L. Cavallo, S. Mecking, J. Am. Chem. Soc. 140 (2017) 1305–1312.
[5] Z. Wang, Q. Liu, G.A. Solan, W.H. Sun, Coord. Chem. Rev. 350 (2017) 68–83.
[6] J.C. Jenkins, M. Brookhart, Organometallics 22 (2003) 250–256.
[7] C. Chen, S.J. Luo, R.F. Jordan, J. Am. Chem. Soc. 130 (2008) 12892–12893.
[8] C. Chen, S.J. Luo, R.F. Jordan, J. Am. Chem. Soc. 132 (2010) 5273–5284.
[9] C. Chen, R.F. Jordan, J. Am. Chem. Soc. 132 (2010) 10254–10255.
[10] Z. Ye, L. Xu, Z. Dong, P. Xiang, Chem. Commun. 49 (2013) 6235–6255.
[11] T. Vaidya, K. Klimovica, A.M. LaPointe, I. Keresztes, E.B. Lobkovsky, O. Daugulis, G.W. Coates, J. Am. Chem. Soc. 136 (2014) 7213–7216.
[12] Z. Jian, L. Falivene, G. Boffa, S. Ortega Sánchez, L. Caporaso, A. Grassi, S. Mecking, Angew. Chem. Int. Ed. 55 (2016) 14378–14383.
[13] Z. Chen, M.D. Leatherman, O. Daugulis, M. Brookhart, J. Am. Chem. Soc. 139 (2017), 16013-10622.
[14] L.H. Guo, W. Liu, C.L. Chen, Mater. Chem. Front. 1 (2017) 2487–2494.
[15] C.L. Chen, ACS Catal. 8 (2018) 5506–5514.
[16] Y. Mitsushige, H. Yasuda, B.P. Carrow, S. Ito, M. Kobayashi, T. Tayano, Y. Watanabe, Y. Okuno, S. Hayashi, J. Kuroda, Y. Okumura, K. Nozaki, ACS Macro Lett. 7 (2018) 305–311.
[17] C.L. Chen, Nat. Rev. Chem. 2 (2018) 6–14.
[18] D.H. Camacho, E.V. Salo, J.W. Ziller, Z. Guan, Angew. Chem. Int. Ed. 43 (2004) 1821–1825.
[19] F.S. Liu, H.B. Hu, Y. Xu, L.H. Guo, S.B. Zai, K.M. Song, H.Y. Gao, L. Zhang, F.M. Zhu, Q. Wu, Macromolecules 42 (2009) 7789–7796.
[20] F.Z. Wang, R. Tanaka, Q.S. Li, Y. Nakayama, T. Shiono, Organometallics 37 (2018) 1358–1367.
[21] L.H. Guo, C.L. Chen, Sci. China Chem. 58 (2015) 1663–1673.
[22] X.L. Sui, S.Y. Dai, C.L. Chen, ACS Catal. 5 (2015) 5932–5937.
[23] F.Z. Wang, R. Tanaka, Z.G. Cai, Y. Nakayama, T. Shiono, Macromol. Rapid Commun. 37 (2016) 1375–1381.
[24] W.P. Zou, C.L. Chen, Organometallics 35 (2016) 1794–1801.
[25] Q. Mahmood, Y.N. Zeng, X.X. Wang, Y. Sun, W.H. Sun, Dalton Trans. 46 (2017) 6934–6947.
[26] X.L. Sui, C.W. Hong, W.M. Pang, C.L. Chen, Mater. Chem. Front. 1 (2017) 967–972.
[27] M.H. Zhao, C.L. Chen, ACS Catal. 7 (2017) 7490–7494.
[28] W.Y. Li, L.H. Guo, W.M. Li, Mol. Catal. 433 (2017) 122–127.
[30] B.P. Yang, S.Y. Xiong, C.L. Chen, Polym. Chem. 8 (2017) 6272–6276.
[31] D. Zhang, C.L. Chen, Angew. Chem. Int. Ed. 56 (2017) 14672–14676.
[32] P.J. Ji, L.H. Guo, X.H. Hu, W.M. Li, J. Polym. Res. 24 (2017) 30.
[33] C. Zou, W. Pang, C.L. Chen, Sci. China Chem. 61 (2018) 1175–1178.
[34] M. Chen, C.L. Chen, Angew. Chem. Int. Ed. 57 (2018) 3094–3098.
[35] L.H. Guo, K.B. Lian, W.Y. Kong, S. Xu, G.R. Jiang, S.Y. Dai, Organometallics 37 (2018) 2442–2449.
[36] C. Zou, S.Y. Dai, C.L. Chen, Macromolecules 51 (2018) 49–56.
[37] S.X. Zhou, C.L. Chen, Sci. Bull. 63 (2018) 441–445.
[38] G.Z. Song, L.H. Guo, Q. Du, W.Y. Kong, W.M. Li, Z. Liu, J. Organomet. Chem. 858 (2018) 1–7.
[39] L.H. Guo, S.Y. Dai, C.L. Chen, Polymers 8 (2016) 37.
[40] S.Y. Dai, C.L. Chen, Macromolecules 51 (2018) 6818–6824.
[41] D.F. Zhang, E.T. Nadres, M. Brookhart, O. Daugulis, Organometallics 32 (2013) 5136–5143.
[42] F.Z. Wang, J.C. Yuan, Q.S. Li, R. Tanaka, Y. Nakayama, T. Shiono, Appl. Organomet. Chem. 28 (2014) 477–483.
[43] F.Z. Wang, R. Tanaka, Q.S. Li, J.C. Yuan, Y. Nakayama, T. Shiono, J. Mol. Catal. Chem. 398 (2015) 231–240.
[44] B.K. Long, J.M. Eagan, M. Mulzer, G.W. Coates, Angew. Chem. Int. Ed. 55 (2016) 7222–7226.
[45] S.Y. Dai, X.L. Sui, C.L. Chen, Angew. Chem. Int. Ed. 54 (2015) 9948–9953.
[46] S.Y. Dai, C.L. Chen, Angew. Chem. Int. Ed. 55 (2016) 13281–13285.
[47] L.H. Guo, C. Zou, S.Y. Dai, C.L. Chen, Polymers 9 (2017) 122.
[48] M. Li, X.B. Wang, Y. Luo, C.L. Chen, Angew. Chem. Int. Ed. 56 (2017) 11604–11609.
[49] F.Z. Wang, R. Tanaka, Z.G. Cai, Y. Nakayama, T. Shiono, Polymer 127 (2017) 88–100.
[50] K. Lian, Y. Zhu, W. Li, S.Y. Dai, C.L. Chen, Macromolecules 50 (2017) 6074–6080.
[51] Y.N. Na, S.Y. Dai, C.L. Chen, Macromolecules 51 (2018) 4040–4048.
[52] J. Fang, X.L. Sui, Y.G. Li, C.L. Chen, Polym. Chem. 9 (2018) 4143–4149.
[53] T.V. Laine, K. Lappalainen, J. Liimatta, E. Aitola, B. Löfgren, M. Leskelä, Macromol. Rapid Commun. 20 (1999) 487–491.
[54] T.V. Laine, U. Piironen, K. Lappalainen, M. Klinga, E. Aitola, M. Leskelä, J. Organomet. Chem. 606 (2000) 112–114.
[55] R.M. Bellabarba, P.T. Gomes, S.I. Pascu, Dalton Trans. 3 (2003) 4431–4436.
[56] W.H. Sun, S. Song, B. Li, C. Redshaw, X. Hao, Y.S. Li, F. Wang, Dalton Trans. 41 (2012) 11999–12010.
[57] H. Suo, T. Zhao, Y. Wang, Q. Ban, W.H. Sun, Molecules 22 (2017) 630–638.
[58] X.L. Chen, J. Gao, H. Liao, H.Y. Gao, Q. Wu, Chin. J. Polym. Sci. 23 (2017) 1–9.
[59] Z. Chen, K.E. Allen, P.S. White, O. Daugulis, M. Brookhart, Organometallics 35 (2016) 1756–1760.
[60] S.Y. Dai, X.L. Sui, C.L. Chen, Chem. Commun. 52 (2016) 9113–9116.
[61] S. Jie, D. Zhang, T. Zhang, W.H. Sun, J. Chen, Q. Ren, D. Liu, G. Zheng, W. Chen, J. Organomet. Chem. 690 (2005) 1739–1749.
[62] X. Mi, Z. Ma, L.Y. Wang, Y.C. Ke, Y.L. Hu, Macromol. Chem. Phys. 204 (2003) 868–876.
[63] Y.D.M. Champouret, J. Fawcett, W.J. Nodes, K. Singh, G.A. Solan, Inorg. Chem. 45 (2006) 9890–9900.
[64] C.Y. Rong, F. Wang, W. Li, M. Chen, Organometallics 36 (2017) 4458–4464.
[65] M. Gao, S. Du, Q. Ban, Q. Xing, W.H. Sun, J. Organomet. Chem. 798 (2015) 401–407.
[67] F.Z. Wang, R. Tanaka, Z.G. Cai, Y. Nakayama, T. Shiono, Polymers 8 (2016) 160.
[68] F.Z. Wang, R. Tanaka, Z.G. Cai, Y. Nakayama, T. Shiono, Polymer 127 (2017) 88–100.
[69] F.Z. Wang, R. Li, S. Tian, K. Lian, D. Guo, W.M. Li, Appl. Organomet. Chem. 32 (2018) e4298.